Disentangling the Gravitational Symphony

Machine Learning for LISA's Global Fit

Antsa Rasamoela
Research Engineer
Computing/Algorithms/Data Team

WINES

ATIONAL WAVE INF

Motivation

- LISA will detect many overlapping GW signals from different type of source
- Classical Bayesian inference methods are computationally expensive
- Explore deep learning for efficient source separation and sampling

from R. Buscicchio's talk, Toulouse, 10/2024

Challenges in LISA

- Complex noise structures (+glitches and gaps)
- Large number of overlapping sources
- High dimensionality of the model
- Presence of correlated parameters

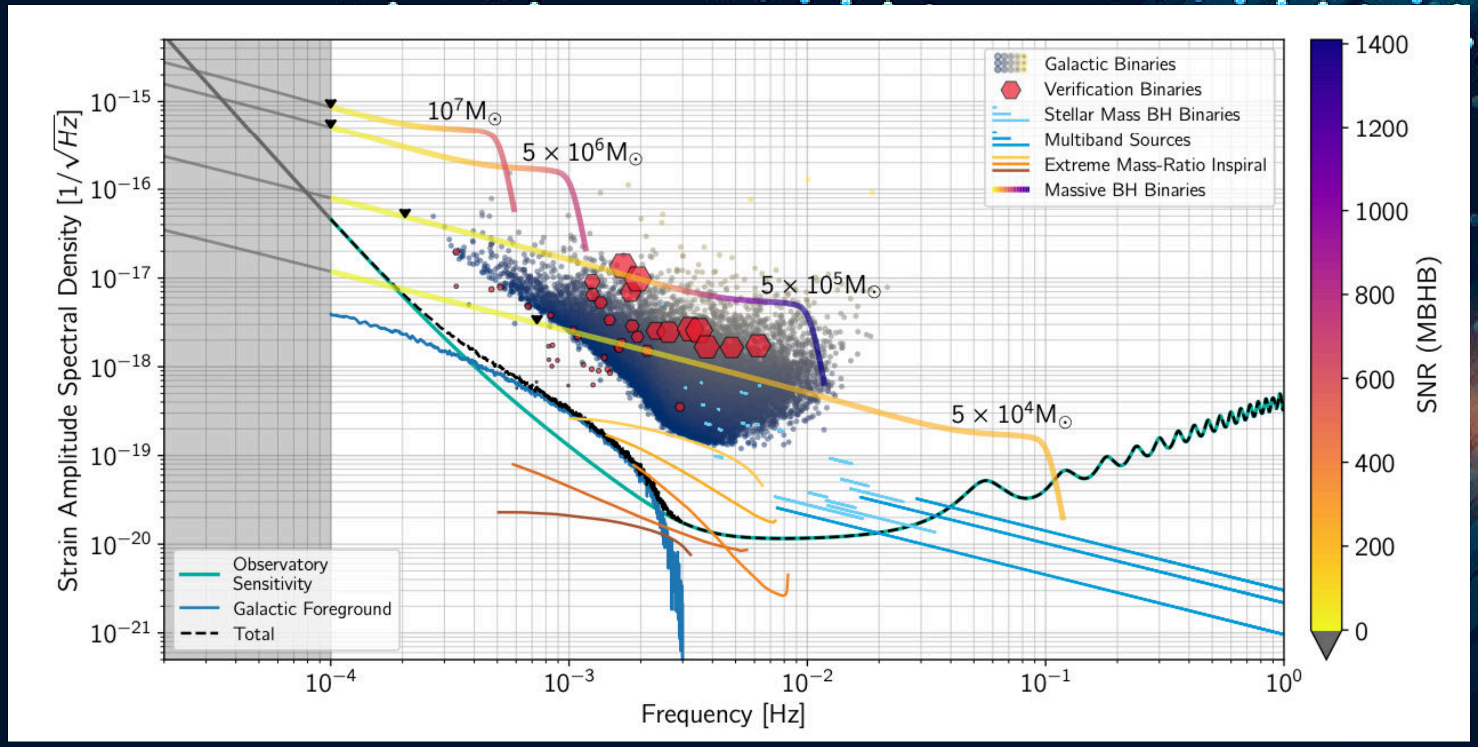

https://arxiv.org/pdf/2402.07571

- GBs : narrow band signals in the frequency domain
- BHBs: transient signals (response varying both with time and freq)
- EMRIs: complex long-lasting signals with low SNR and timescales of several years

GW separation / denoising

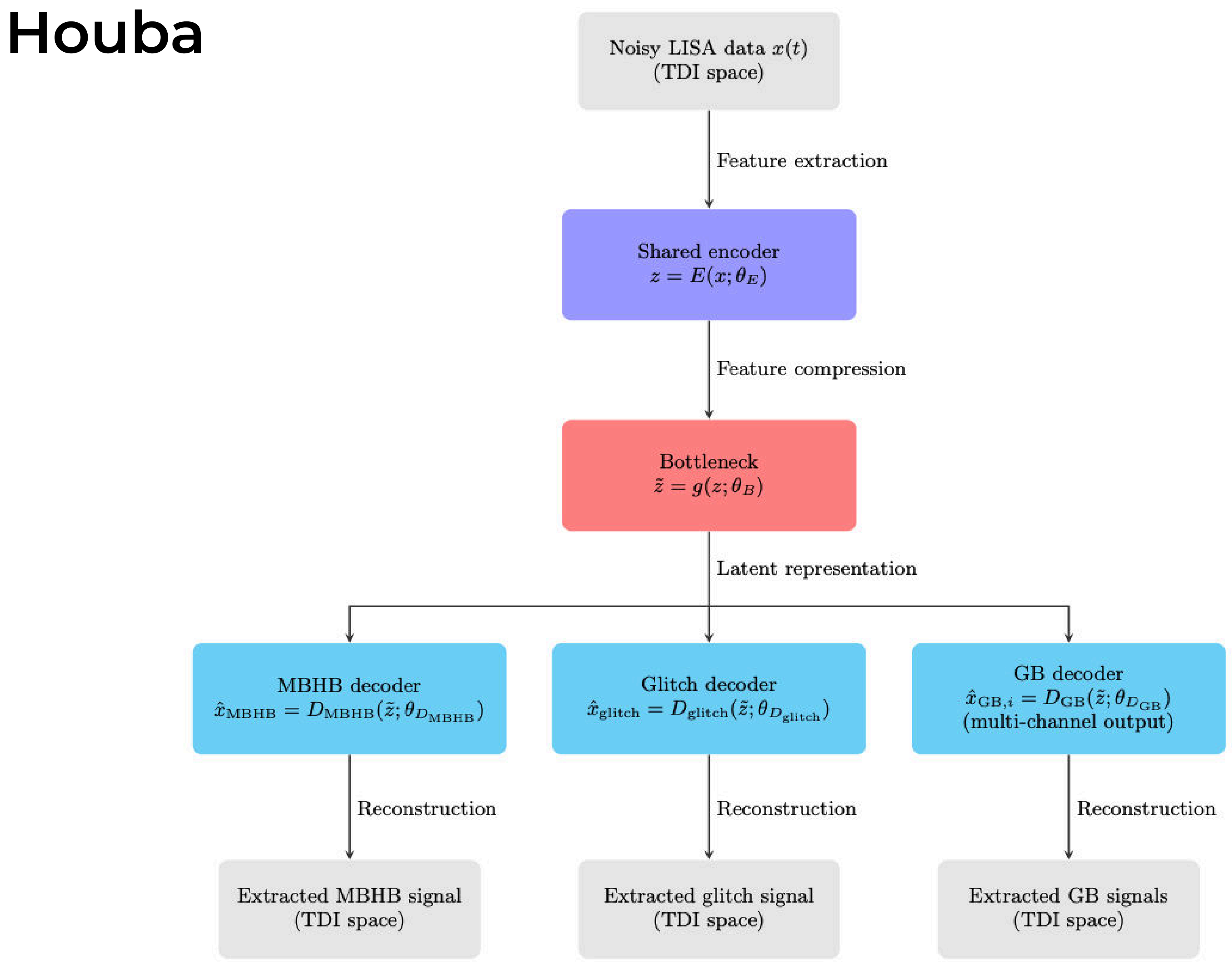

FIG. 2: Deep source separation framework for LISA data, where a shared encoder compresses the TDI input, and decoders reconstruct MBHBs, GBs and glitches. Since the input data denotes a TDI channel, the separated and decoded output signals are represented in the TDI space, as well.

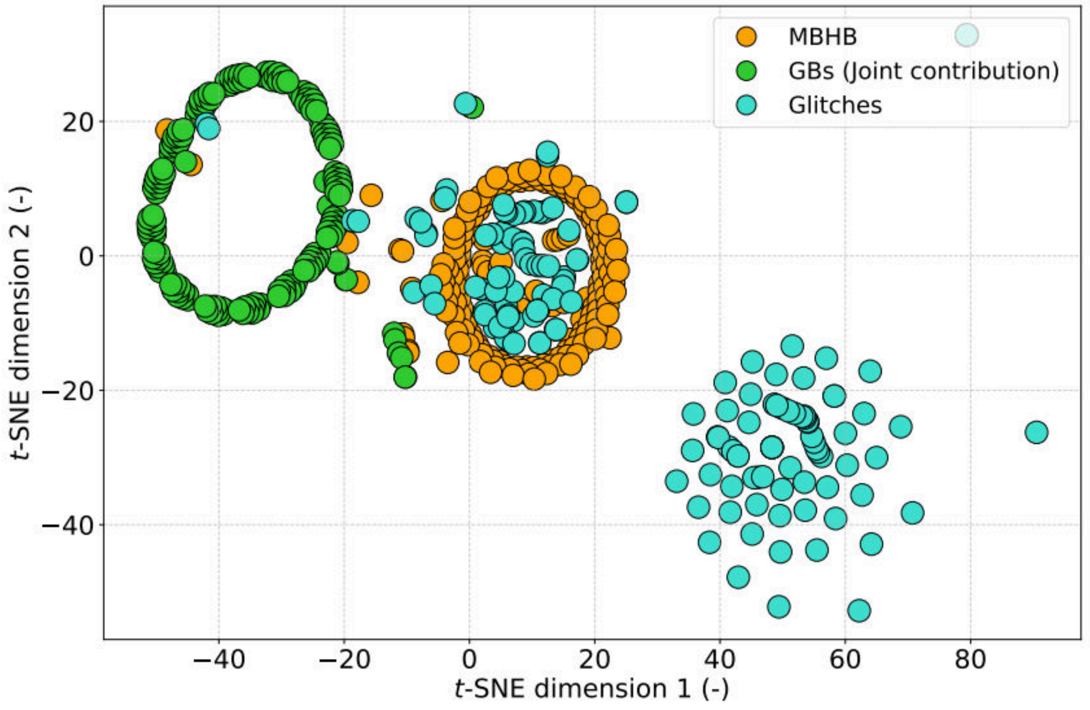

FIG. 4: t-SNE projection of bottleneck-encoded features derived from the normalized time series data in Fig. 3, illustrating clustering of merging MBHBs, GBs, and glitches. Note that separating sources within an abstract feature space beyond traditional temporal and spectral domains denotes a reorientation of methodology in LISA data analysis.

https://arxiv.org/pdf/2503.10398

Bayesian Deep Learning

Denoising Diffusion Restoration Models

	Super-resolution	Inpainting		Deblurring
Observations (Inputs) $\mathbf{y}$				
Outputs from our method $\mathbf{x}_0$				

[NeurIPS 2022] Denoising Diffusion Restoration Models

Applicable to other domains as well!

Speech

A VERSATILE DIFFUSION-BASED GENERATIVE REFINER FOR SPEECH ENHANCEMENT

Ryosuke Sawata, Naoki Murata, Yuhta Takida, Toshimitsu Uesaka, Takashi Shibuya, Shusuke Takahashi, Yuki Mitsufuji

Sony Group Corporation, Tokyo, Japan

UNSUPERVISED VOCAL DEREVERBERATION WITH DIFFUSION-BASED GENERATIVE MODELS

Koichi Saito, Naoki Murata, Toshimitsu Uesaka, Chieh-Hsin Lai, Yuhta Takida, Takao Fukui, Yuki Mitsufuji

Sony Group Corporation, Tokyo, Japan

Bayesian Deep Learning

Denoising Diffusion Restoration Models

	Super-resolution	Inpainting		Deblurring
Observations (Inputs) $\mathbf{y}$				
Outputs from our method $\mathbf{x}_0$				

[NeurIPS 2022] Denoising Diffusion Restoration Models

Applicable to other domains as well!

Astronomy

Strong-Lensing Source Reconstruction with Denoising Diffusion Restoration Models

Ryos

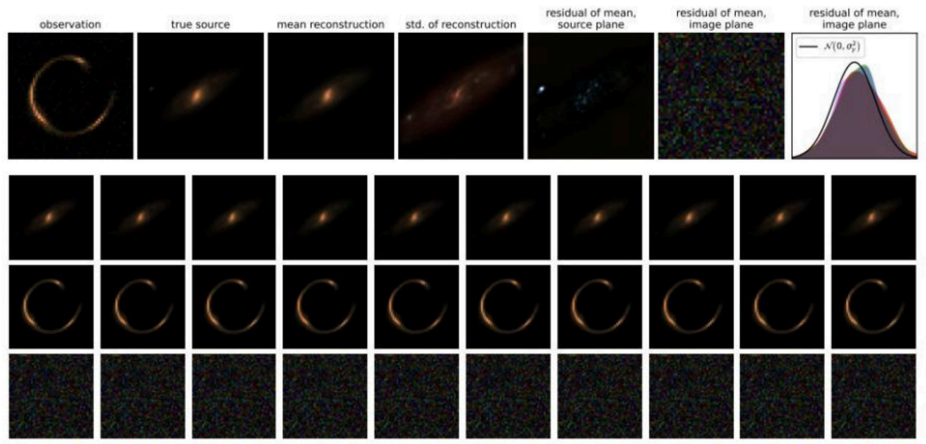

Koic

Figure 1: Top: from left to right, the mock observation, $\mathbf{y}$ (with a medium noise level), the true source, $\mathbf{x}$ (an unconstrained sample from AstroDDPM), the mean and standard deviation of 100 posterior samples from DDRM, $\mathbf{x}_{0,i} \sim p_\Theta(\mathbf{x}_0 \mid \mathbf{y})$, and the residual of the mean with respect to the true source and with respect to the observation in the image plane; finally, a histogram of the latter compared to a Gaussian. Bottom: each column is a random posterior sample (top row), which is then lensed to produce the respective noiseless image $\mathbf{H}\mathbf{x}_{0,i}$ (middle row). Shown (bottom row) are also the residuals between $\mathbf{H}\mathbf{x}_{0,i}$ and the observation. In residual plots, negative values in one channel are shown as positive values in the other two (red ↔ cyan, green ↔ magenta, blue ↔ yellow), considering complementary colors as "negative".

WINESS

AVITATIONAL WAVE INFEREN

RAL SOURCE SEPARATI

- GWINESS project started in January 2025
- Blind source separation of overlapping GWs
- Inspired by music/speech separation

- SCNet deep learning architecture for music source separation in Time-Freq Domain
- DDRM diffusion-based reconstruction model that denoises/samples data (e.g., images)
- SepReformer transformer-based model designed for multi-speaker separation


GWINESS
GRAVITATIONAL WAVE INFERENCE
NEURAL SOURCE SEPARATION
Data Input
Drop HDF5 files here
or
Browse Files
Loaded File:
Name: mixed_test.hdf5
Size: 6.43 GB
Modified: 29/04/2025 16:35:38
Analysis Tools
Spectrogram
Parameter
Correlation
Source Information
MBHB GW150914-like 2.3 Gpc
EMRI Extreme Mass Ratio 4.1 Gpc
Galactic White Dwarf Binary 8 kpc
Visualization Controls
Fullscreen
Item: 10
Start
Stop
Mixed Input
Export
MBHB
Focus
Log Amplitude
Frequency (Hz)
Time (days)
Time Domain
Sampling Rate: 0.1 Hz
Separated Outputs
Hide
All
Show
MBHB Massive Black Hole Binary
SNR: 24.5
Frequency: 0.01-0.1 Hz
EMRI Extreme Mass Ratio Inspiral
SNR: 18.2
Frequency: 0.001-0.01 Hz
Galactic White Dwarf Binary
SNR: 32.7
Frequency: 0.1-1 Hz
Residual Remaining Noise
Power: 0.05
Frequency: Full Band


GWINESS
GRAVITATIONAL WAVE INFERENCE
NEURAL SOURCE SEPARATION
Data Input
Drop HDF5 files here
or
Browse Files
Loaded File:
Name: mixed_test.hdf5
Size: 6.43 GB
Modified: 29/04/2025 16:35:38
Analysis Tools
Spectrogram
Parameter
Correlation
Source Information
MBHB GW150914-like 2.3 Gpc
EMRI Extreme Mass Ratio 4.1 Gpc
Galactic White Dwarf Binary 8 kpc
Visualization Controls
Fullscreen
Item: 42
Start
Stop
Mixed Input
Export
MBHB
Focus
Log Amplitude
Frequency (Hz)
Time (days)
Time Domain
Sampling Rate: 0.1 Hz
Separated Outputs
Hide
All
Show
MBHB Massive Black Hole Binary
SNR: 24.5
Frequency: 0.01-0.1 Hz
EMRI Extreme Mass Ratio Inspiral
SNR: 18.2
Frequency: 0.001-0.01 Hz
Galactic White Dwarf Binary
SNR: 32.7
Frequency: 0.1-1 Hz
Residual Remaining Noise
Power: 0.05
Frequency: Full Band

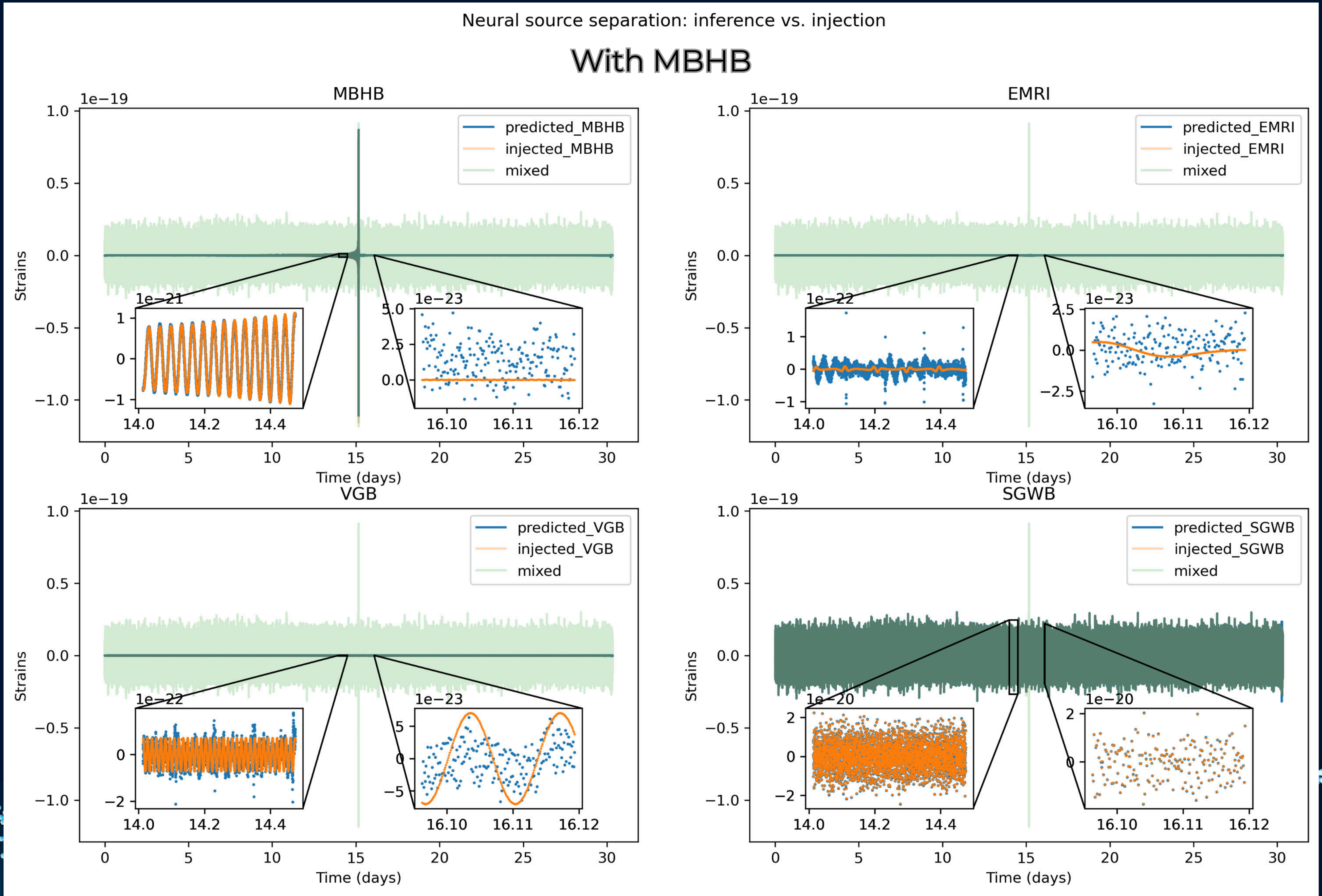

Neural source separation: inference vs. injection
With MBHB
MBHB
EMRI
VGB
SGWB
predicted_MBHB
injected_MBHB
mixed
predicted_EMRI
injected_EMRI
predicted_VGB
injected_VGB
predicted_SGWB
injected_SGWB
Strains
Time (days)
1e−19
1e−21
1e−22
1e−23
1e−20

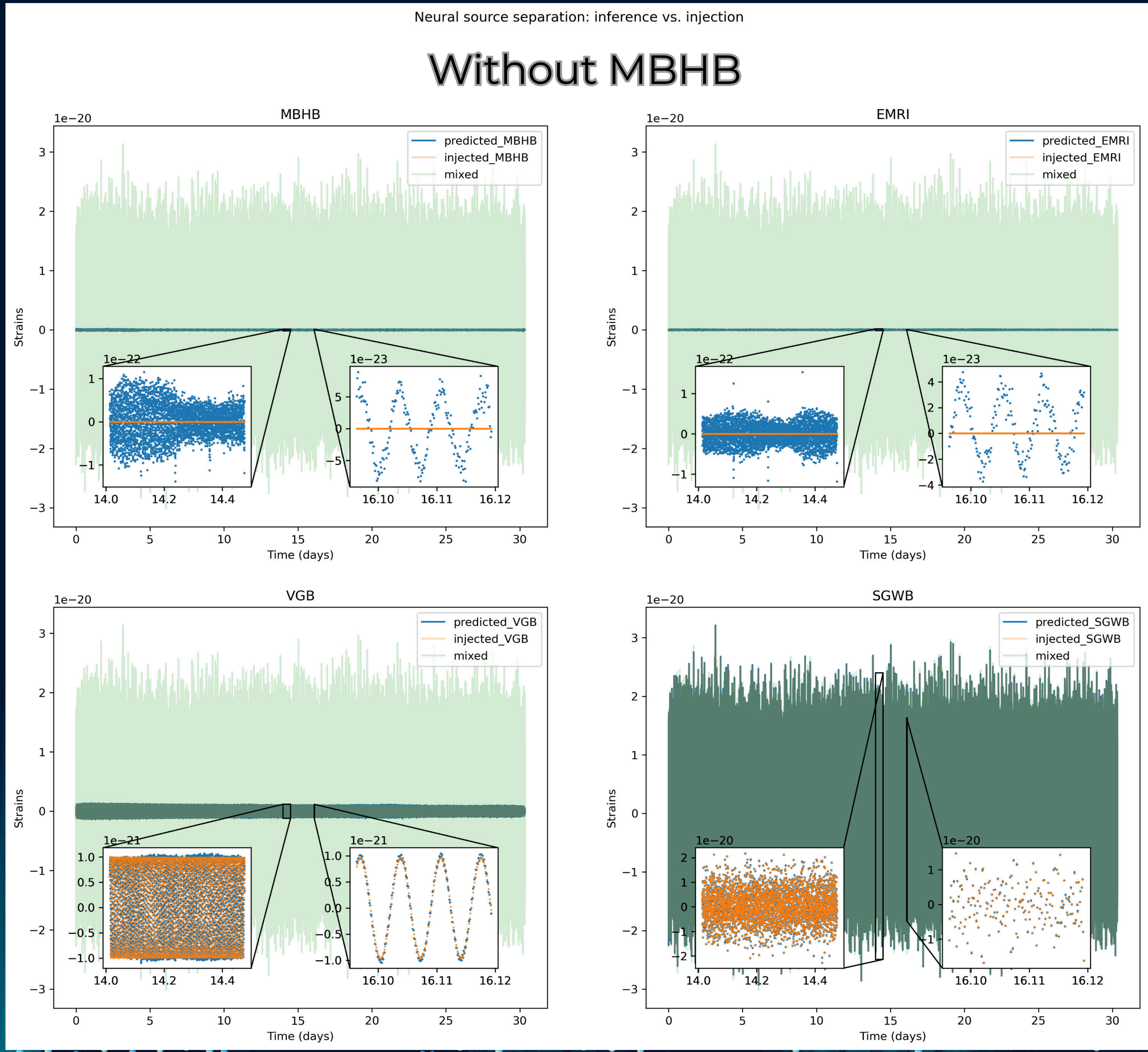
Neural source separation: inference vs. injection
Without MBHB
MBHB
EMRI
VGB
SGWB
predicted_MBHB
injected_MBHB
predicted_EMRI
injected_EMRI
predicted_VGB
injected_VGB
predicted_SGWB
injected_SGWB
mixed
Strains
Time (days)

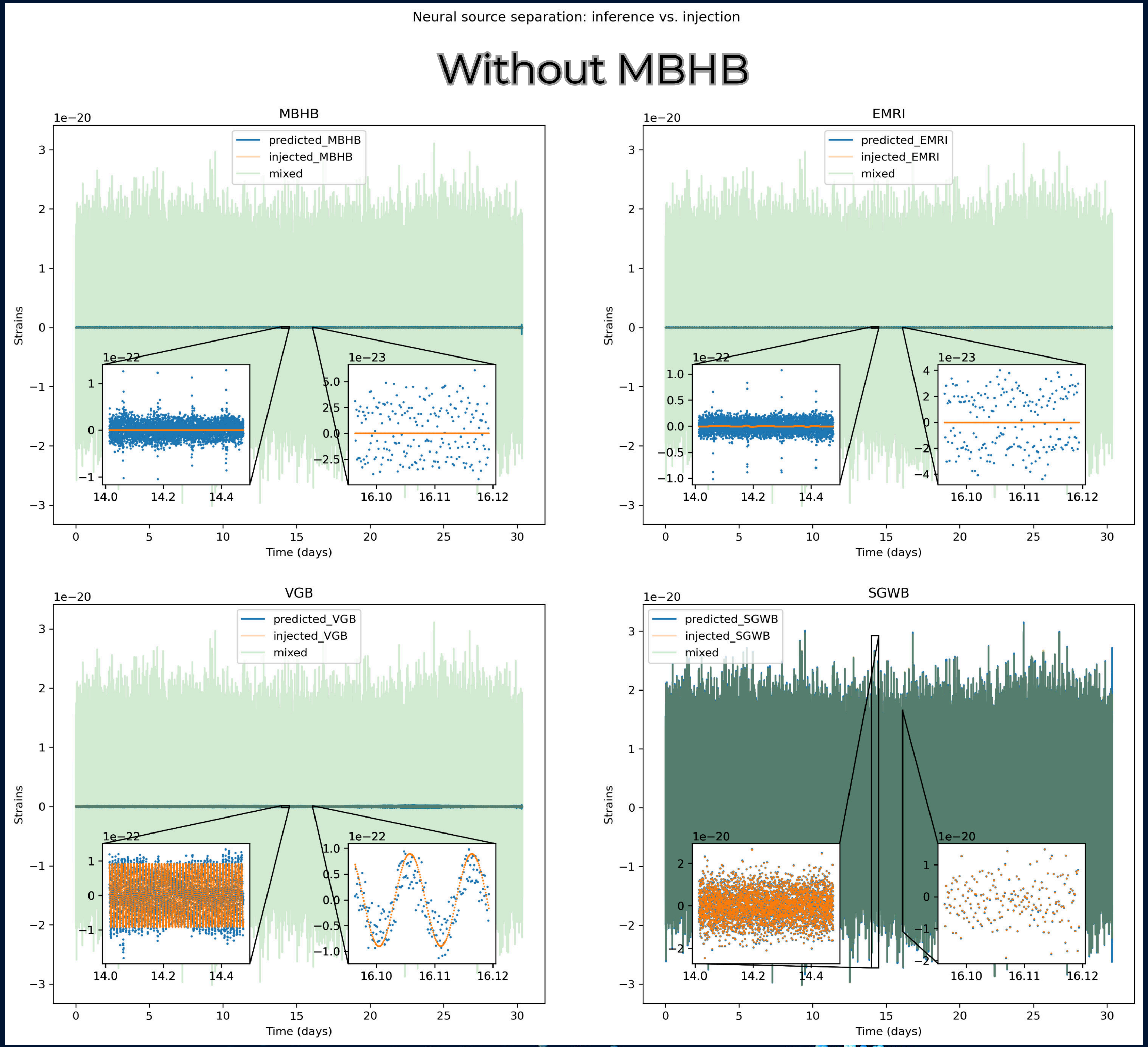
Neural source separation: inference vs. injection
Without MBHB
MBHB
EMRI
VGB
SGWB
predicted_MBHB
injected_MBHB
predicted_EMRI
injected_EMRI
predicted_VGB
injected_VGB
predicted_SGWB
injected_SGWB
mixed
Strains
Time (days)

GWINESS

GRAVITATIONAL WAVE INFERENCE
NEURAL SOURCE SEPARATION

1. Large class-level separation

LISA TDI → SCNet Coarse Separation → Source Type Channels

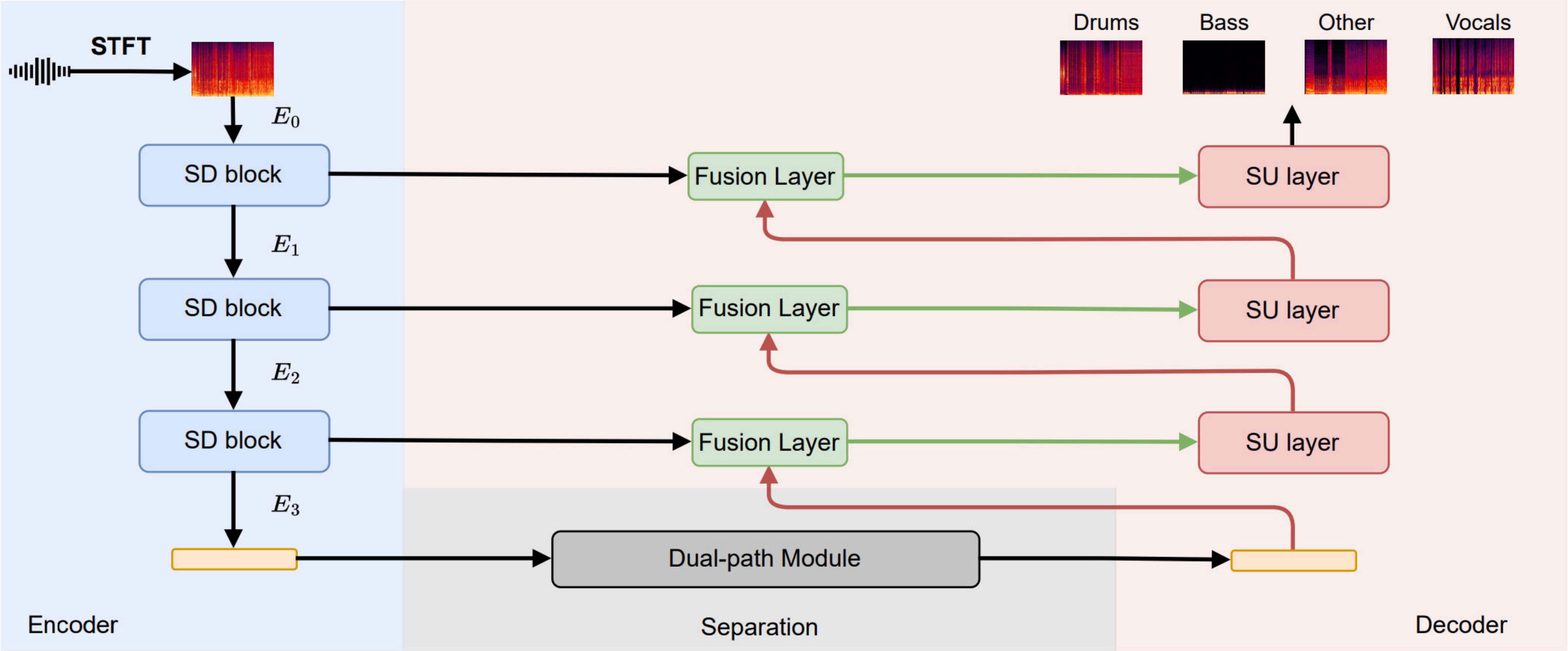

Fig. 1. The overall architecture of SCNet.

https://arxiv.org/pdf/2401.13276

2. Probabilistic refinement

LISA TDI → SCNet Coarse Separation → Source Type Channels

↓

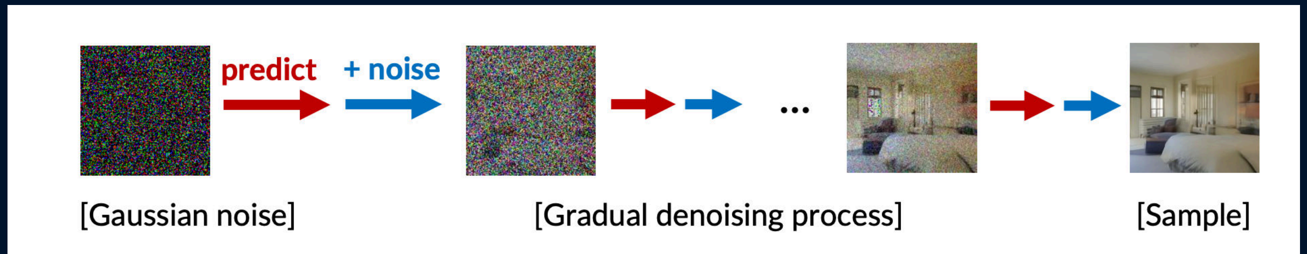

DDRM Denoising / Sampling

↓

Clean Mixture Samples

(per type, e.g., GBs within small frequency windows)

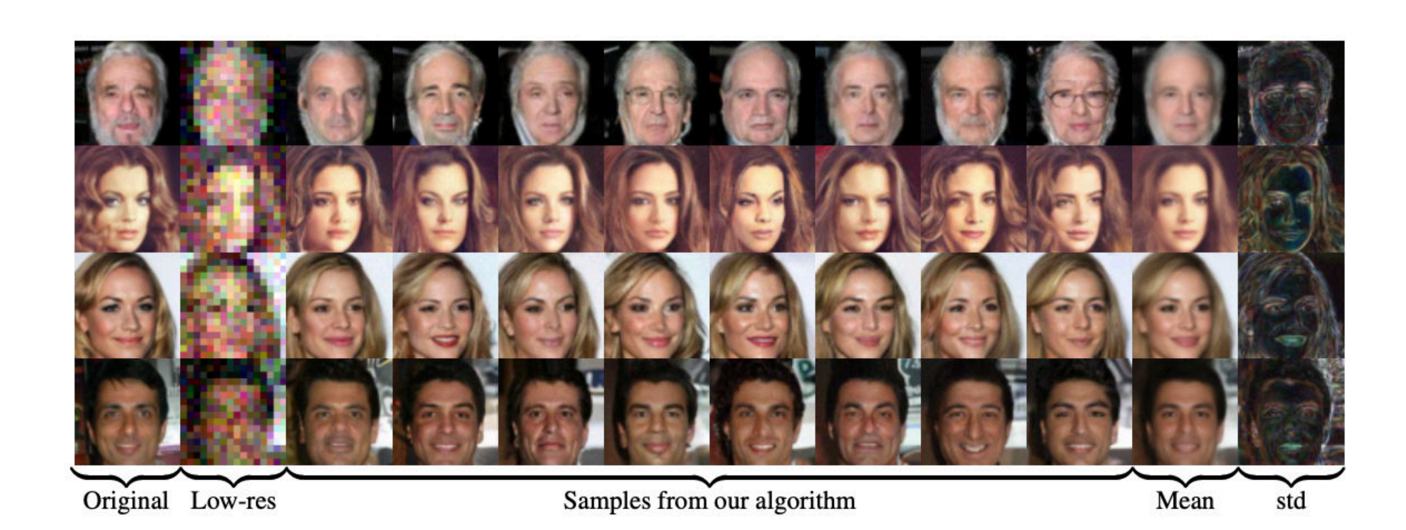

https://arxiv.org/pdf/2105.14951

3. Overlapping sources unmixing

LISA TDI → SCNet Coarse Separation → Source Type Channels

↓

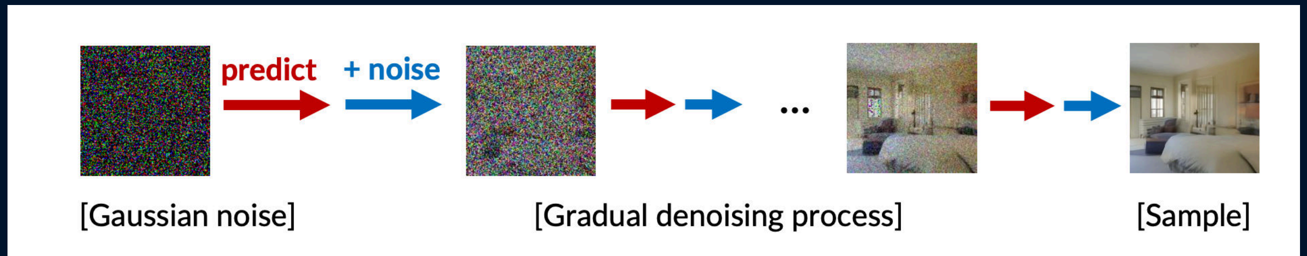

DDRM Denoising / Sampling

↓

Clean Mixture Samples

↓

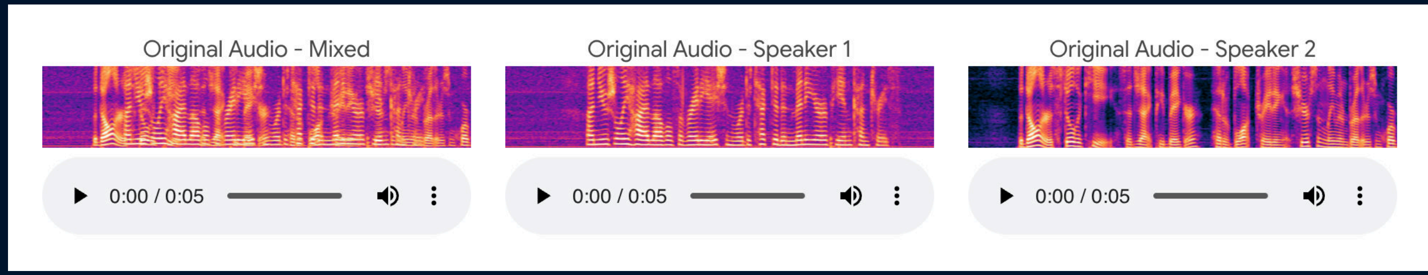

SepReformer Fine Separation

↓

Clean Waveform Samples $\{source_1, \ldots, source_n\}$

3. Overlapping sources unmixing

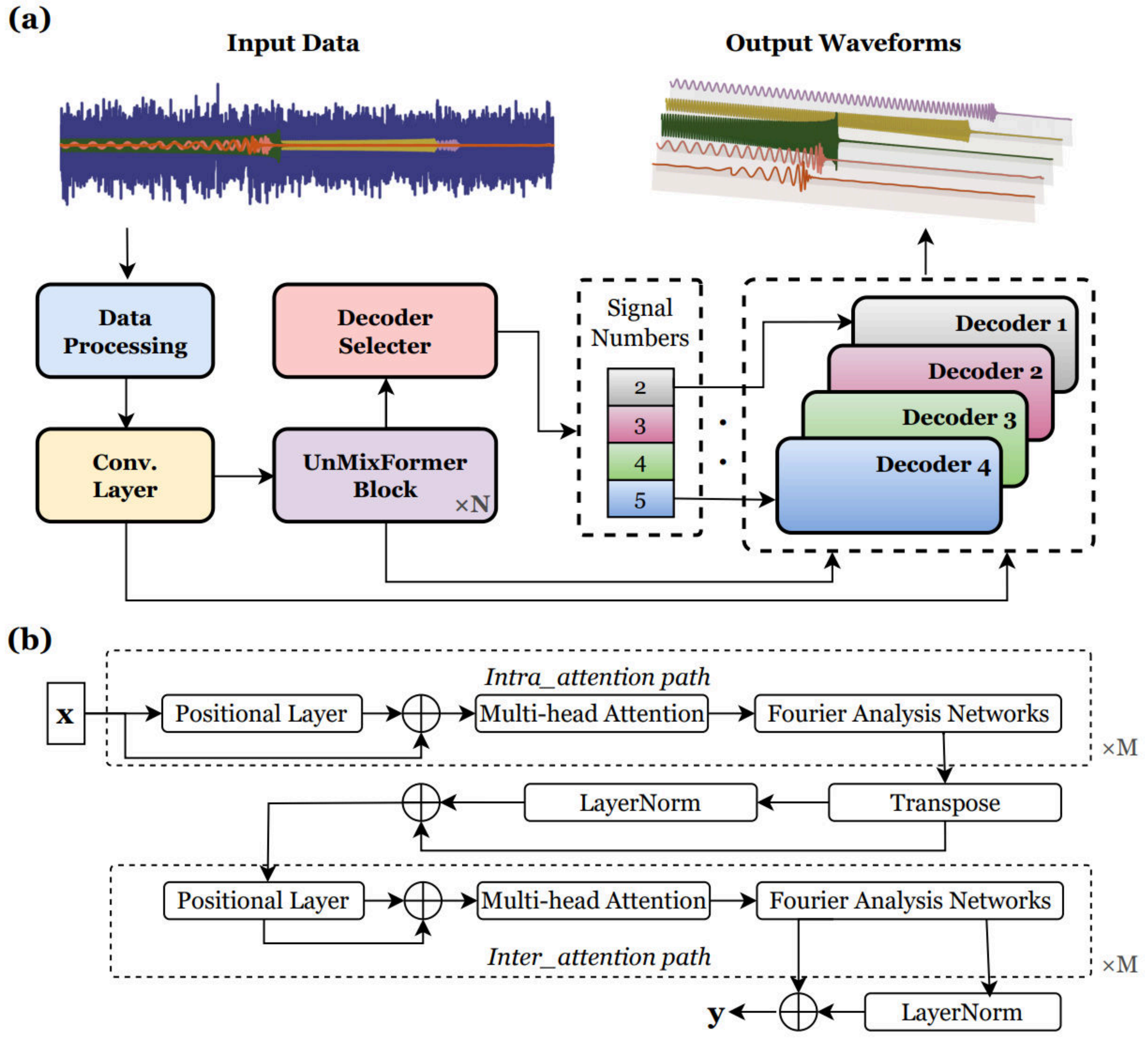

Figure 2. **UnMixFormer Architecture.** (a). The overall framework for counting and separating overlapping GW signals. We firstly employ CNN-based encoders to extract data embeddings, which are then fused and passed into UnMixFormer blocks. The counting head predicts the number of sources and activates the appropriate decoder to reconstruct individual waveforms. (b). The core UnMixFormer block operates with intra- and inter-attention mechanisms to capture fine-grained local features and global context. FAN layers in the feedforward module enhance periodic feature modeling and the positional encoding incorporates sequential information, enabling efficient separation of overlapping signals.

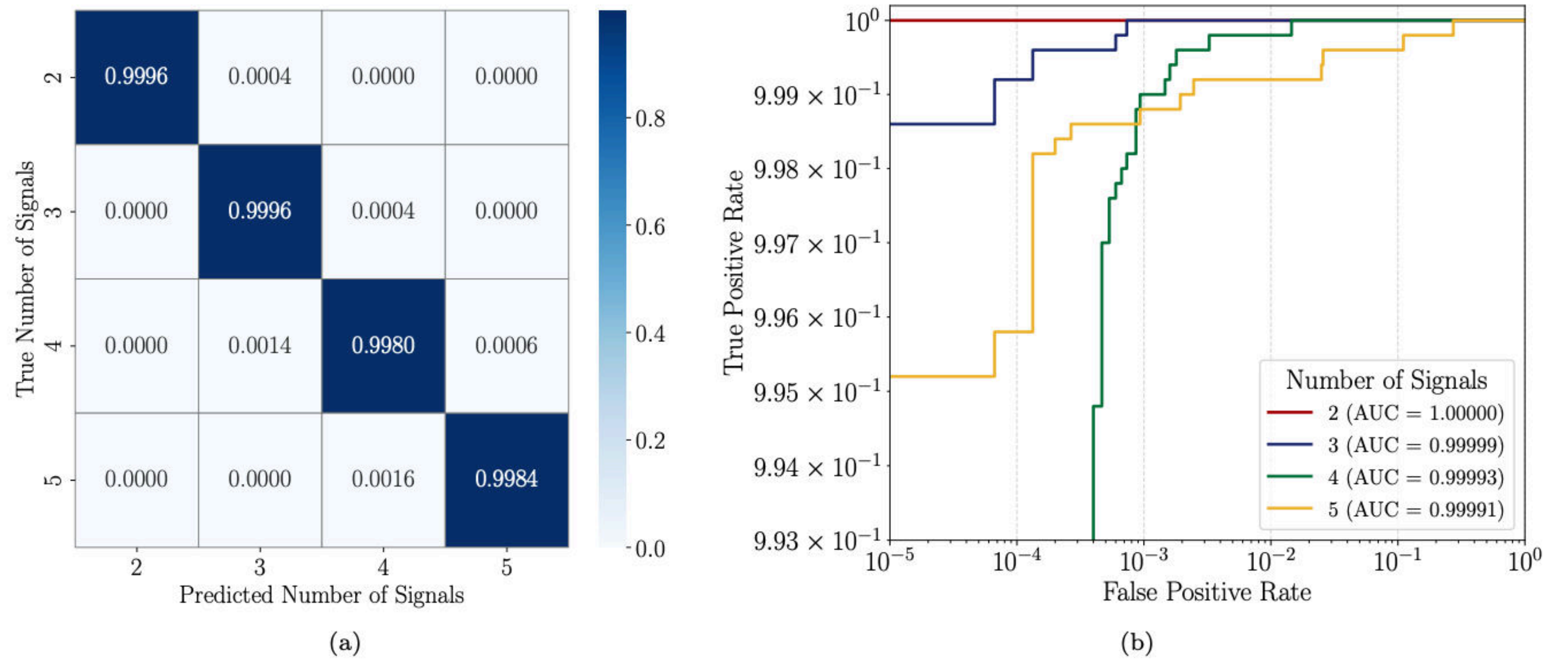

Figure 3. **Counting performance of overlapping CBC signals.** (a). The normalized confusion matrix shows the high accuracy of predicting the number of overlapping signals, with correct predictions dominating the diagonal entries (2 to 5 signals). (b). ROC curves illustrating the performance of signal counting for varying numbers of signals. The curves demonstrate near-perfect detection across all cases.

https://arxiv.org/pdf/2412.18259

GWINESS

GRAVITATIONAL WAVE INFERENCE
NEURAL SOURCE SEPARATION

Integration to L2D roadmap

Timeline

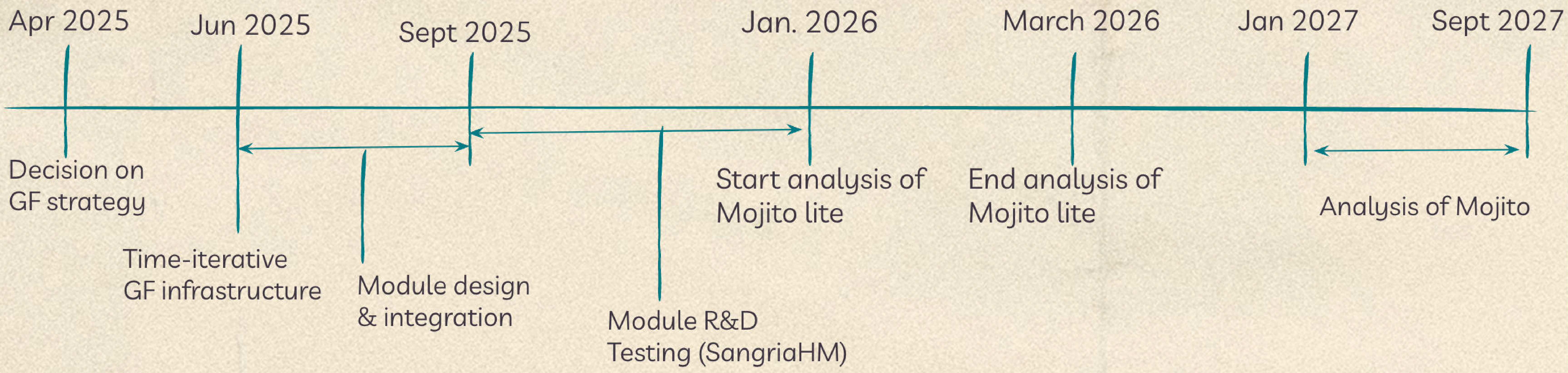

Future directions

While the benefits are clear, there are also many challenges to consider:

- working on a proof of concept
- !!! looking for collaboration !!!
- quality assurance / acceptable AI

The GWINESS approach requires further investigation:

- dataset generation during training (many overlapping sources)
- hyperparameter tuning
- test with parameter estimation

Data quality and computational resources impact its effectiveness:

- implement fast waveform generator for L2A / L2D (CU-WAV?)
- develop training dataset pipeline for L2A / L2D (CU-SIM?)
- need a GPU-based cluster suited for large model training (SysTeam?)

MeLisa Project

A Machine Learning toolkit for LISA

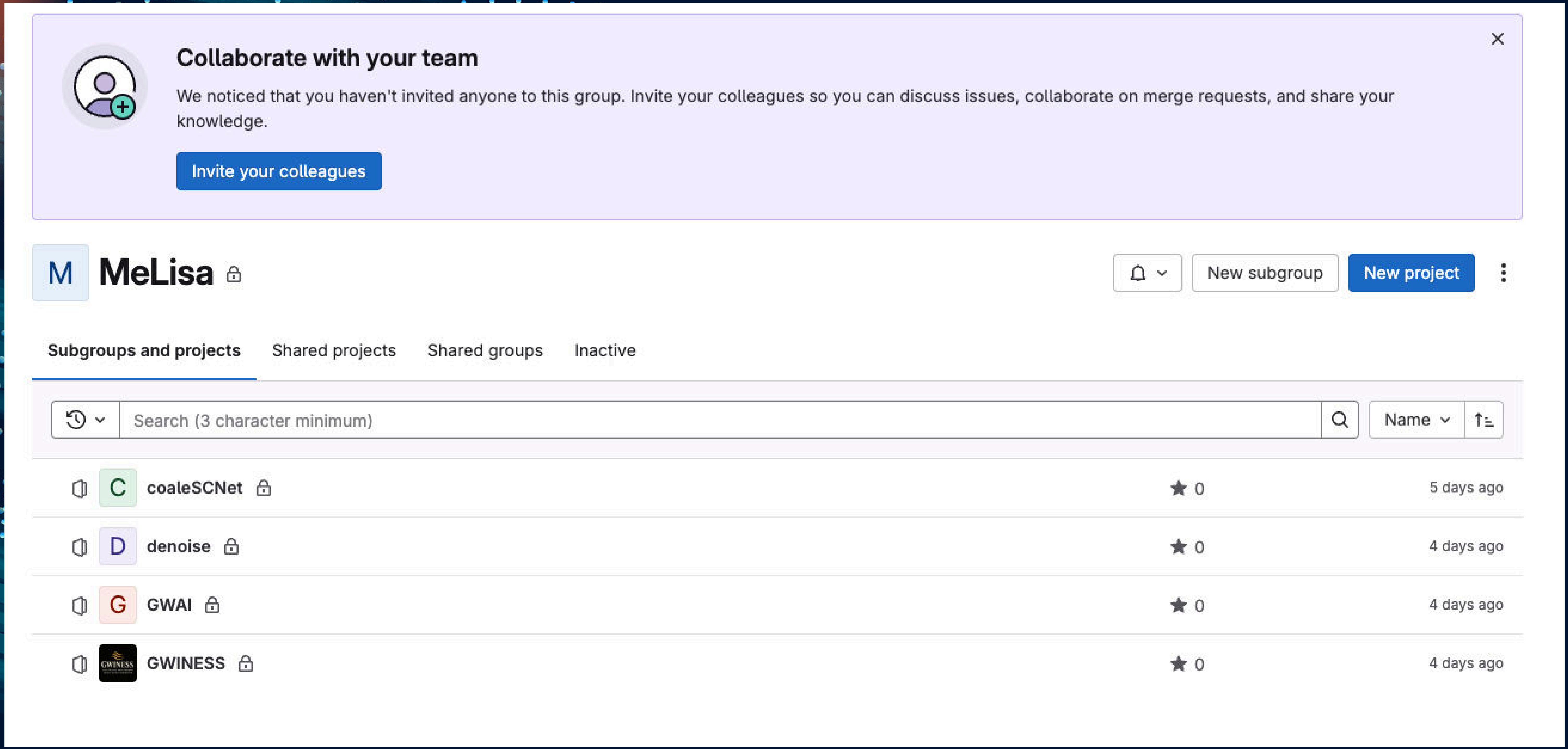

Thanks!

Do you have any questions?

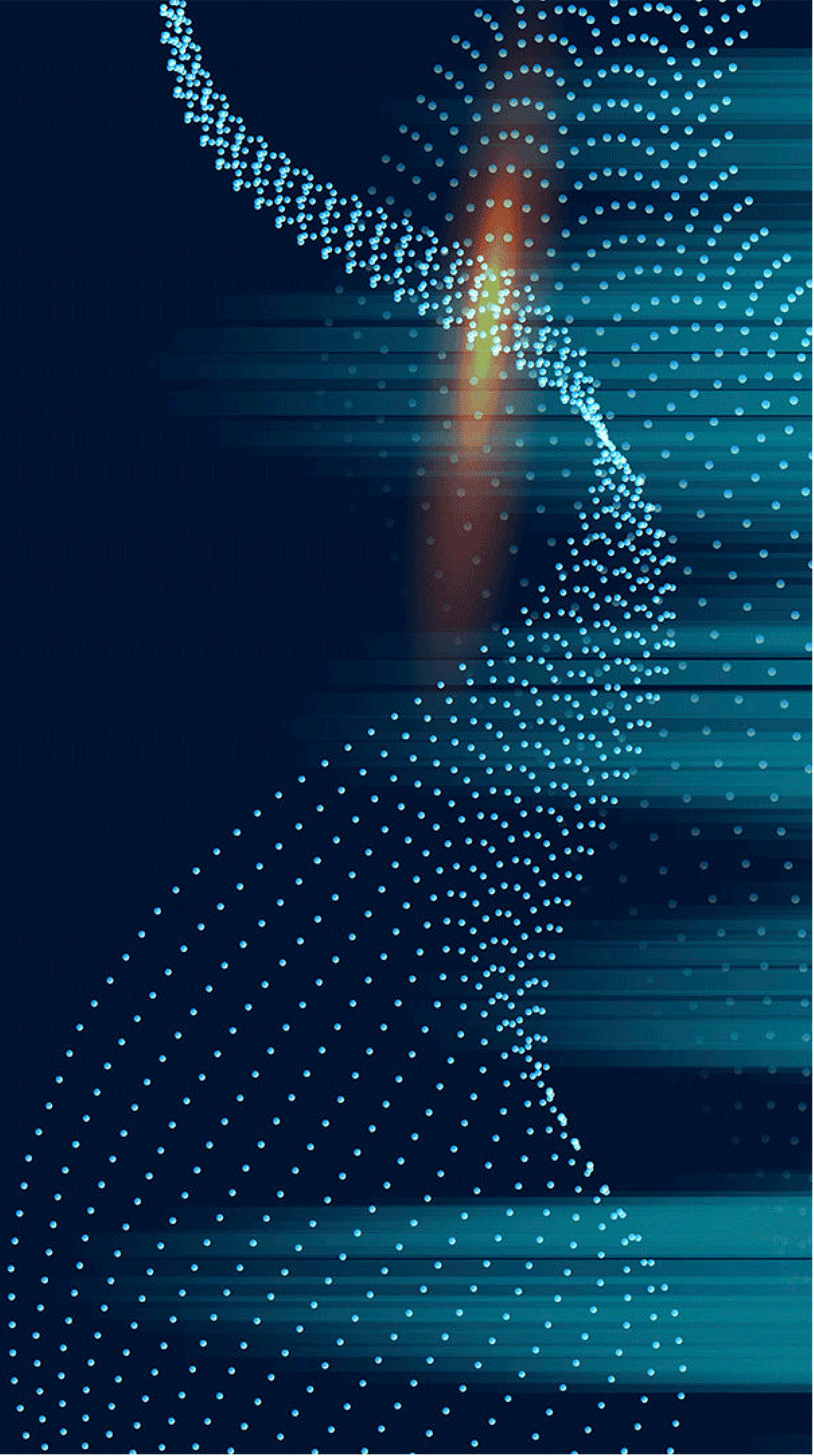

Neural source separation: inference vs. injection

With MBHB

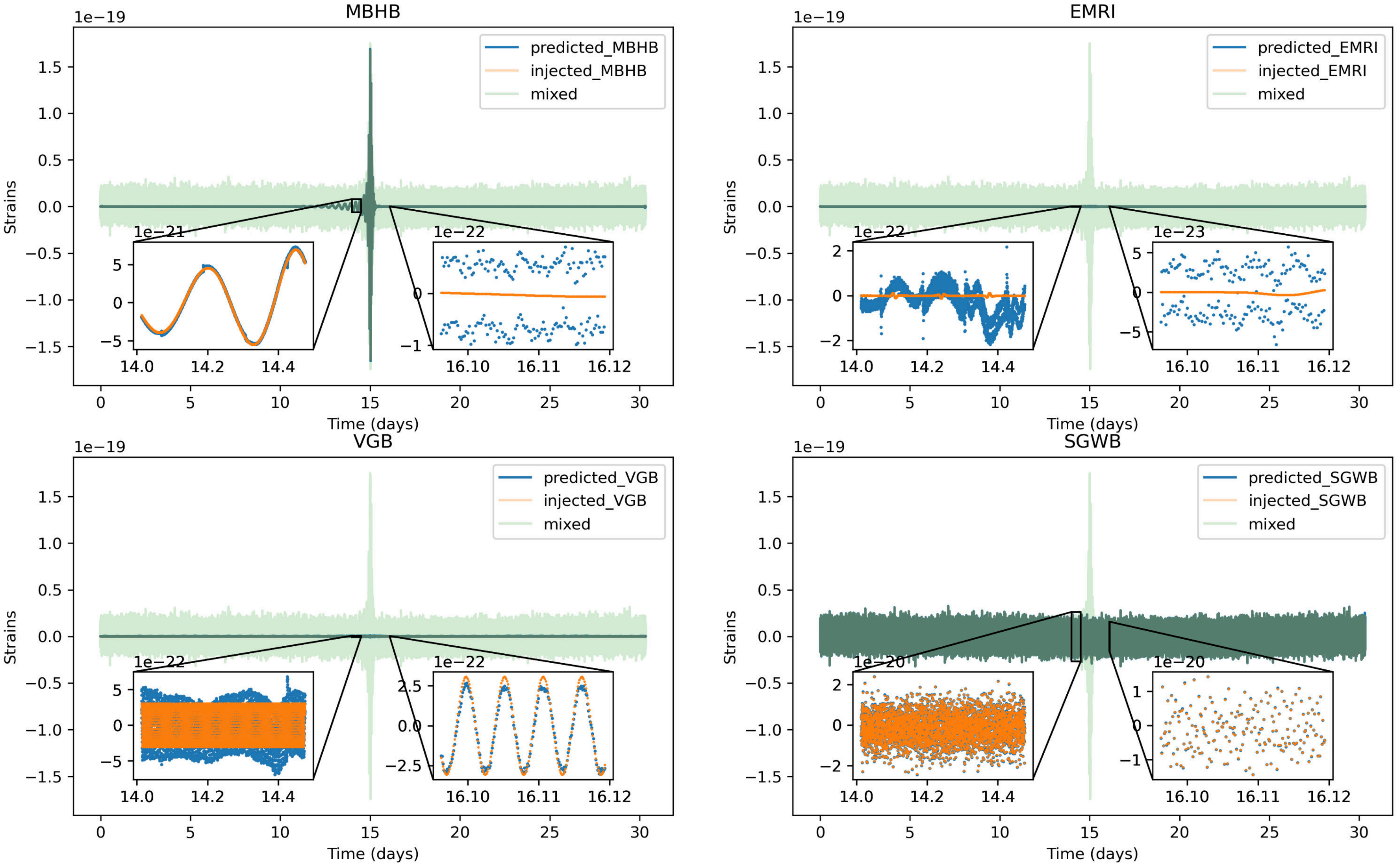

Neural source separation: inference vs. injection

Without MBHB

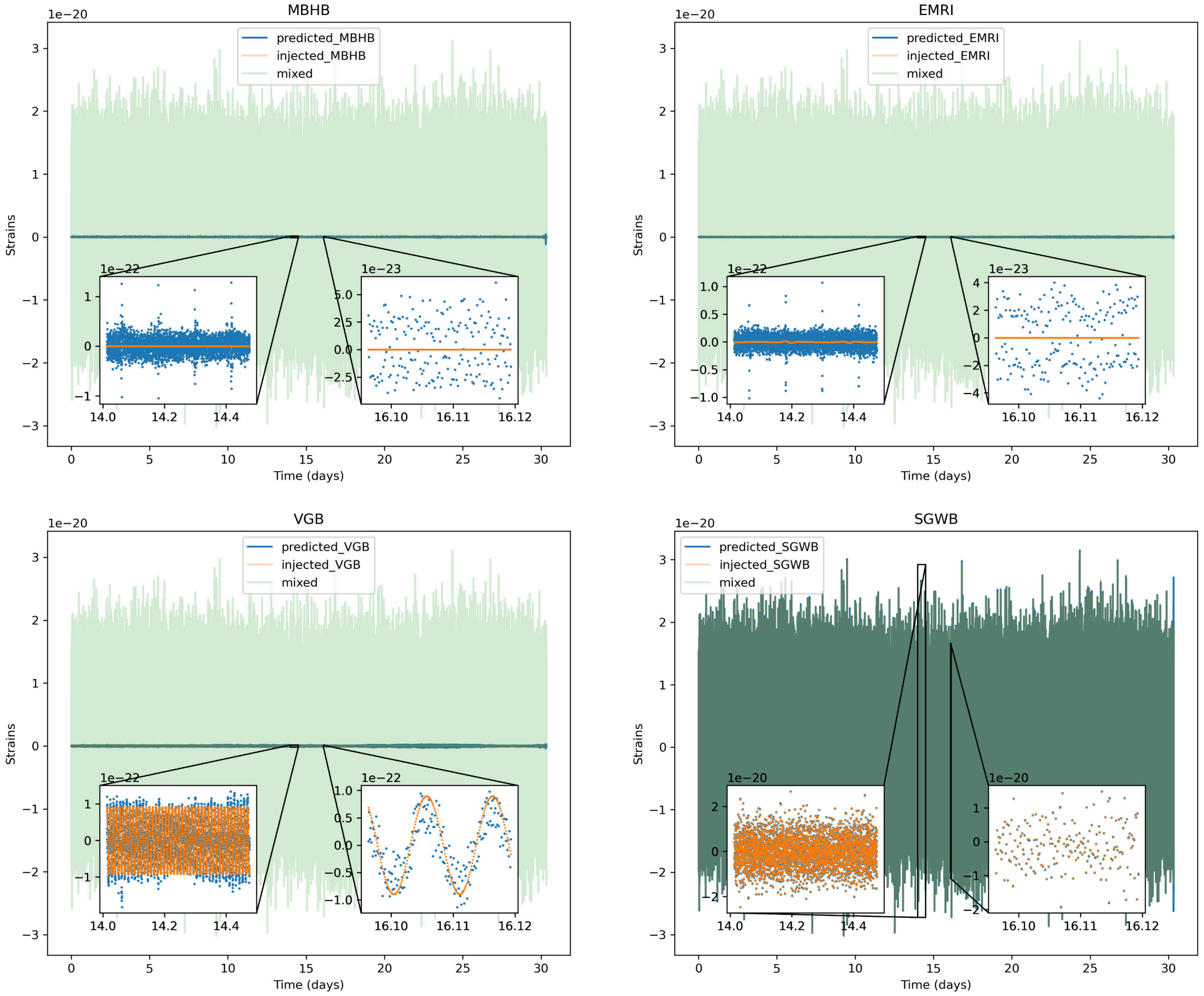

Signal denoising

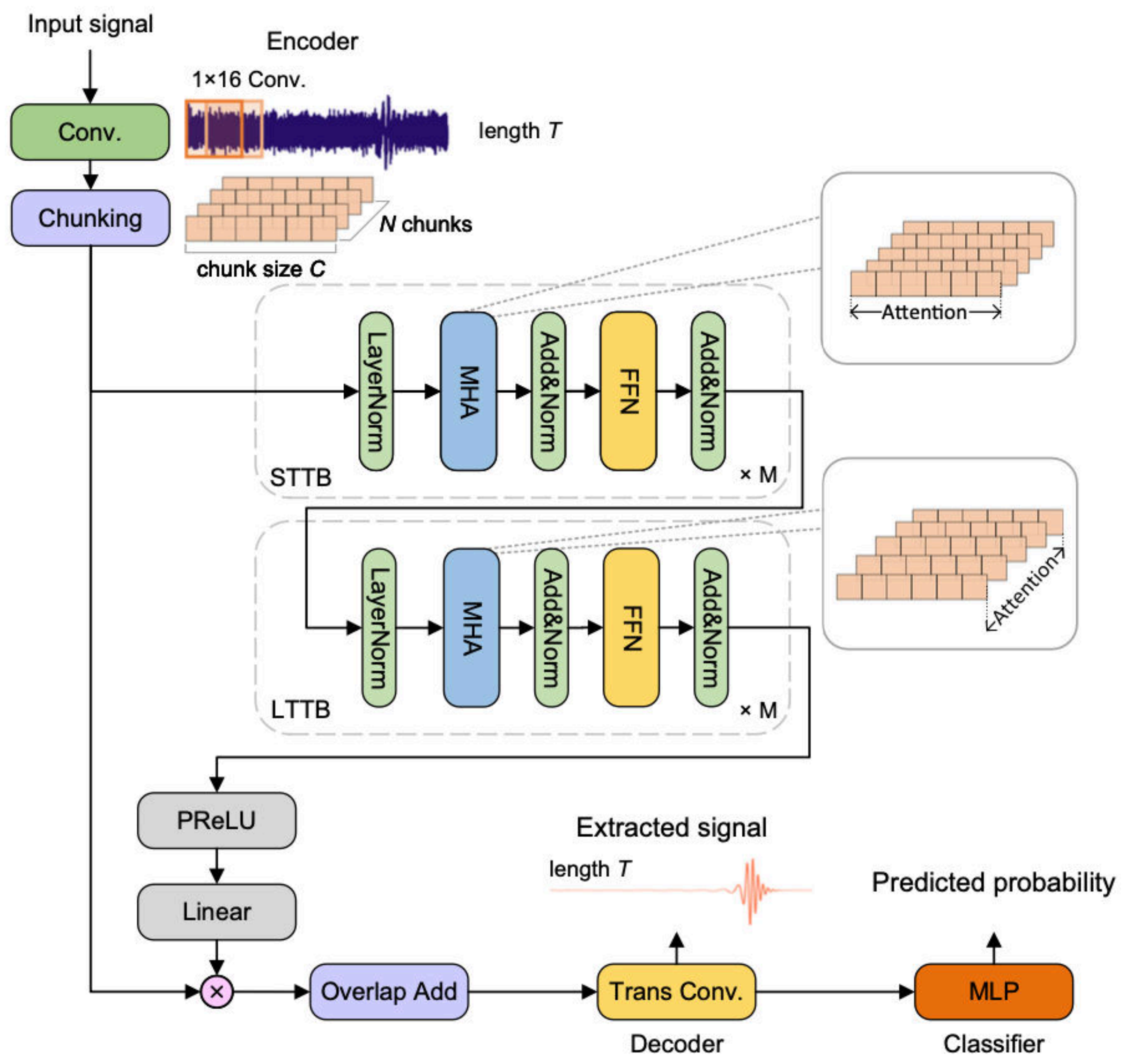

Fig. 1 The overall architecture of our Transformer based deep neural network. Beginning with a convolutional network-based encoder, data is transformed and feed into the Transformer-based extraction network. This network composed of several Short-Term Transformer Blocks (STTB) and Long-Term Transformer Blocks (LTTB), excels in capturing both local and global dependencies within the GW data, aimed at extracting GW signals. The final stage is a multi-layer perception-based classifier, responsible for the signal detection and provide a predicted probability.

Table 1 Summary of parameter setups in EMRI signal simulation.

Parameter	Lower bound	Upper bound
M	$10^5 M_\odot$	$10^7 M_\odot$
a	10^{-3}	0.99
e_0	10^{-3}	0.5
$\cos\iota$	-1	1

Table 2 Summary of parameter setups in MBHB signal simulation.

Parameter	Lower bound	Upper bound
M_{tot}	$10^6 M_\odot$	$10^8 M_\odot$
q	0.01	1
s_1^z	-0.99	0.99
s_2^z	-0.99	0.99

Table 3 Summary of parameter setups in BWD signal simulation.

Parameter	f	$\dot{f}$
Range-1	$[0.1, 4]$mHz	$[-3\times10^{-17}, 6\times10^{-16}]\mathrm{Hz}^2$
Range-2	$[4, 15]$mHz	$[-3\times10^{-15}, 4\times10^{-14}]\mathrm{Hz}^2$

https://www.nature.com/articles/s42005-023-01334-6

Signal denoising & separation

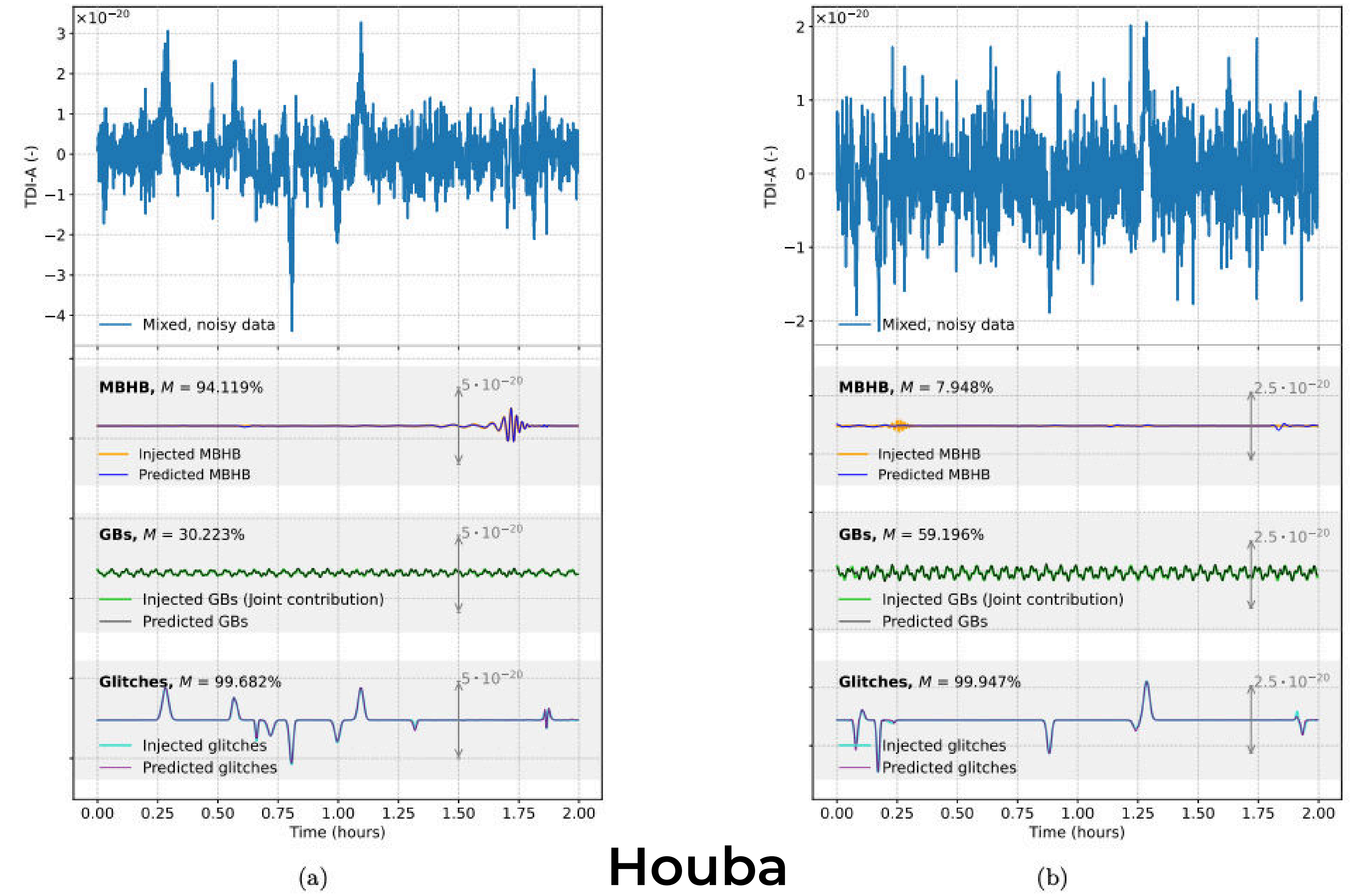

Houba

FIG. 7: Comparison of injected waveforms and model predictions for a low-amplitude MBHB merger buried in stationary noise. In panel (a), the deep source separation framework successfully detects and reconstructs the MBHB signal. However, in (b), where the signal amplitude is further diminished, the model fails. In such cases, further investigation is needed to determine whether the issue lies in the shared encoder or the MBHB decoder head.

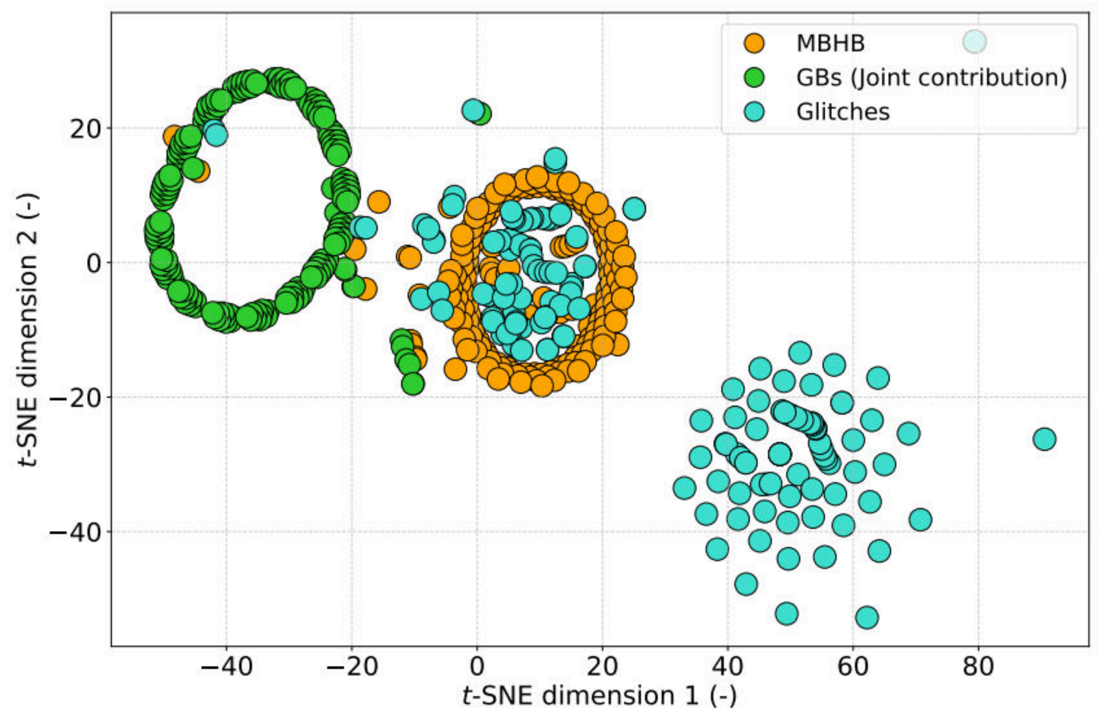

FIG. 4: t-SNE projection of bottleneck-encoded features derived from the normalized time series data in Fig. 3, illustrating clustering of merging MBHBs, GBs, and glitches. Note that separating sources within an abstract feature space beyond traditional temporal and spectral domains denotes a reorientation of methodology in LISA data analysis.

https://arxiv.org/pdf/2503.10398

Signal denoising & separation

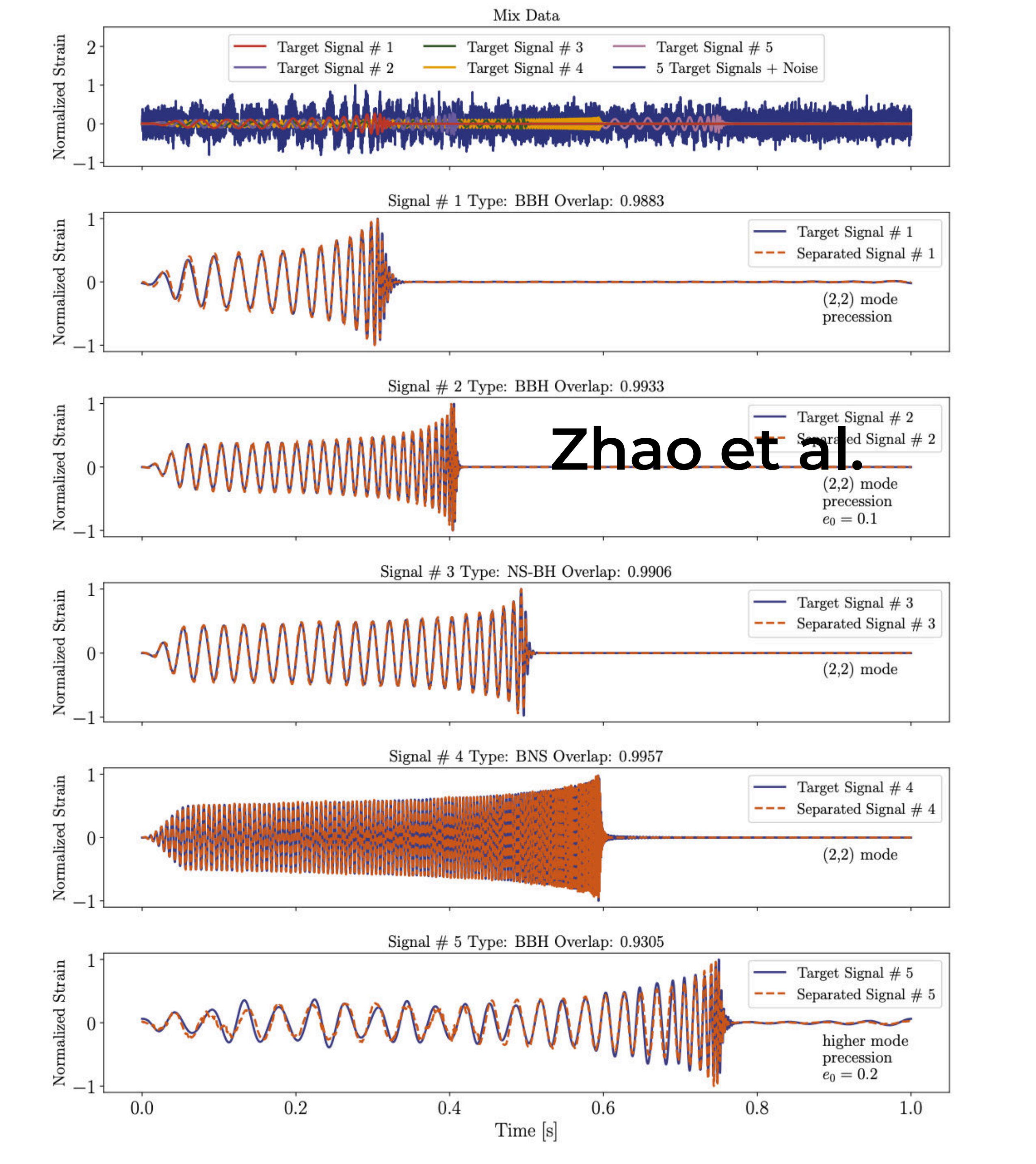

Figure 5. **Showcase of signal separation and generalization ability.** The top panel illustrates the mixed data that contains five target signals burried in noise. Other panels display the separated individual signals and target templates, including BBH waveforms with precession, orbital eccentricity, and higher modes, as well as NS-BH and BNS waveforms. The overlaps between the separated and target signals are consistently high, demonstrating the model's effectiveness in separating different types of signals and generalizing to diverse complex waveforms.

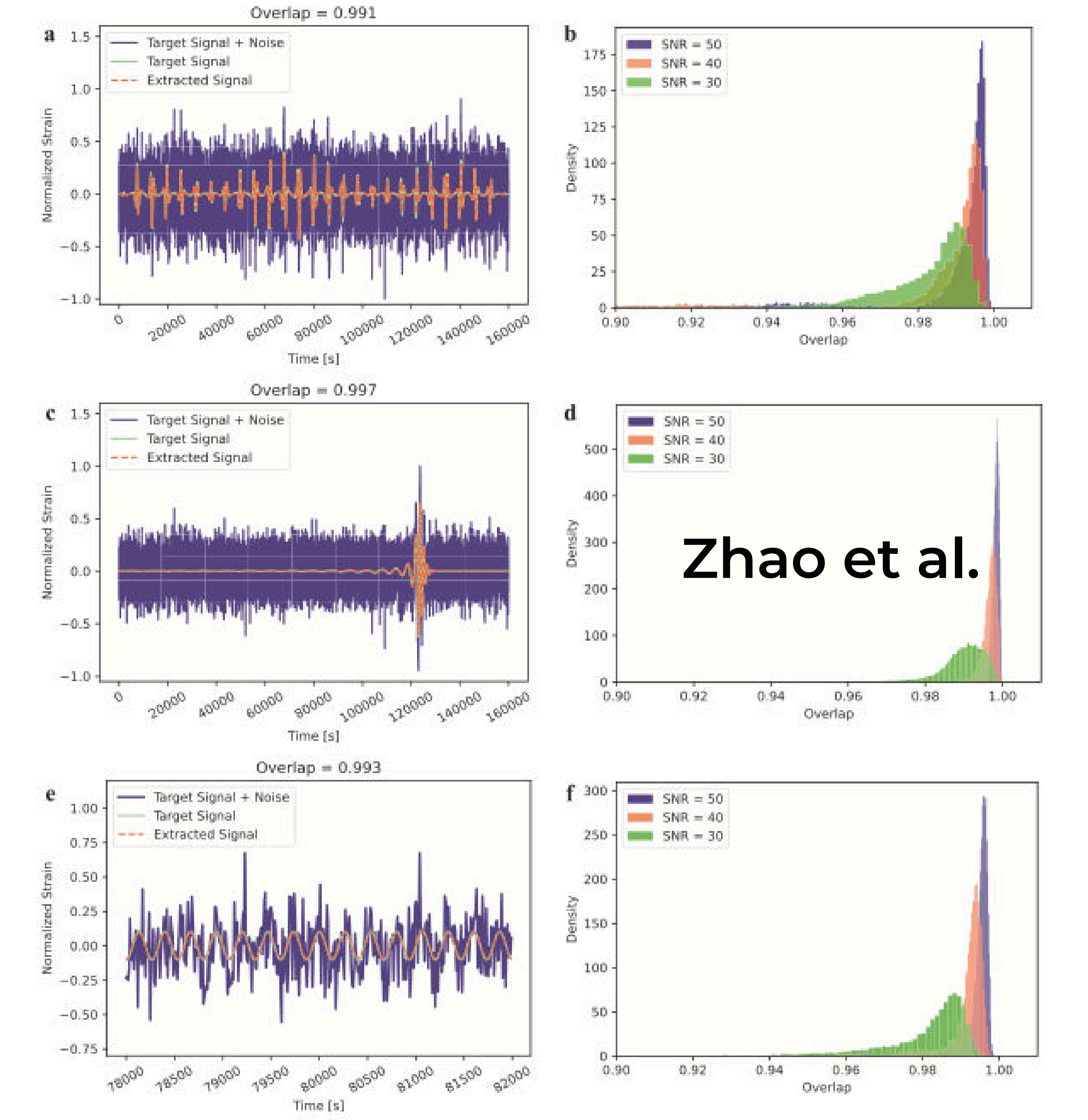

Fig. 4 The signal extraction examples and the overlapping (between the target and extracted signals) distributions for different GW sources. a and **b** EMRI. **c** and **d** MBHB. **e** and **f** BWD. The extracted signal is compared with whitened templates. Only the middle part of the BWD waveform is presented to show the details of the waveform. The overlap between extracted data and waveform templates is shown on the top. The high values indicate the strong performance of our method on signal extraction for different GW sources. Tests on different signal SNRs also show our models' generalization ability.

https://arxiv.org/pdf/2412.18259

https://www.nature.com/articles/s42005-023-01334-6

Signal denoising & separation

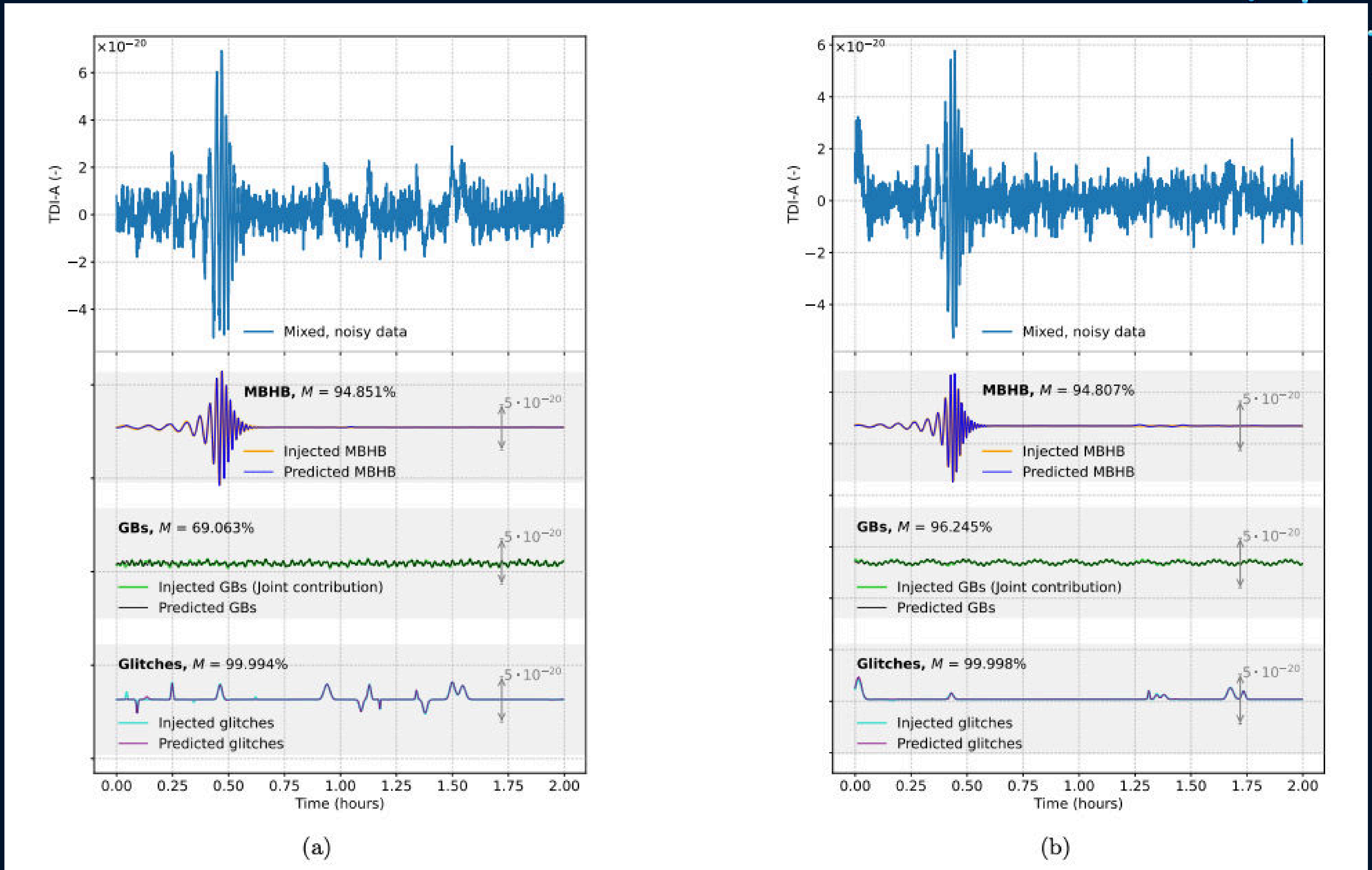

when glitches overlap with the MBHB merger phase

https://arxiv.org/pdf/2503.10398

Signal denoising & separation

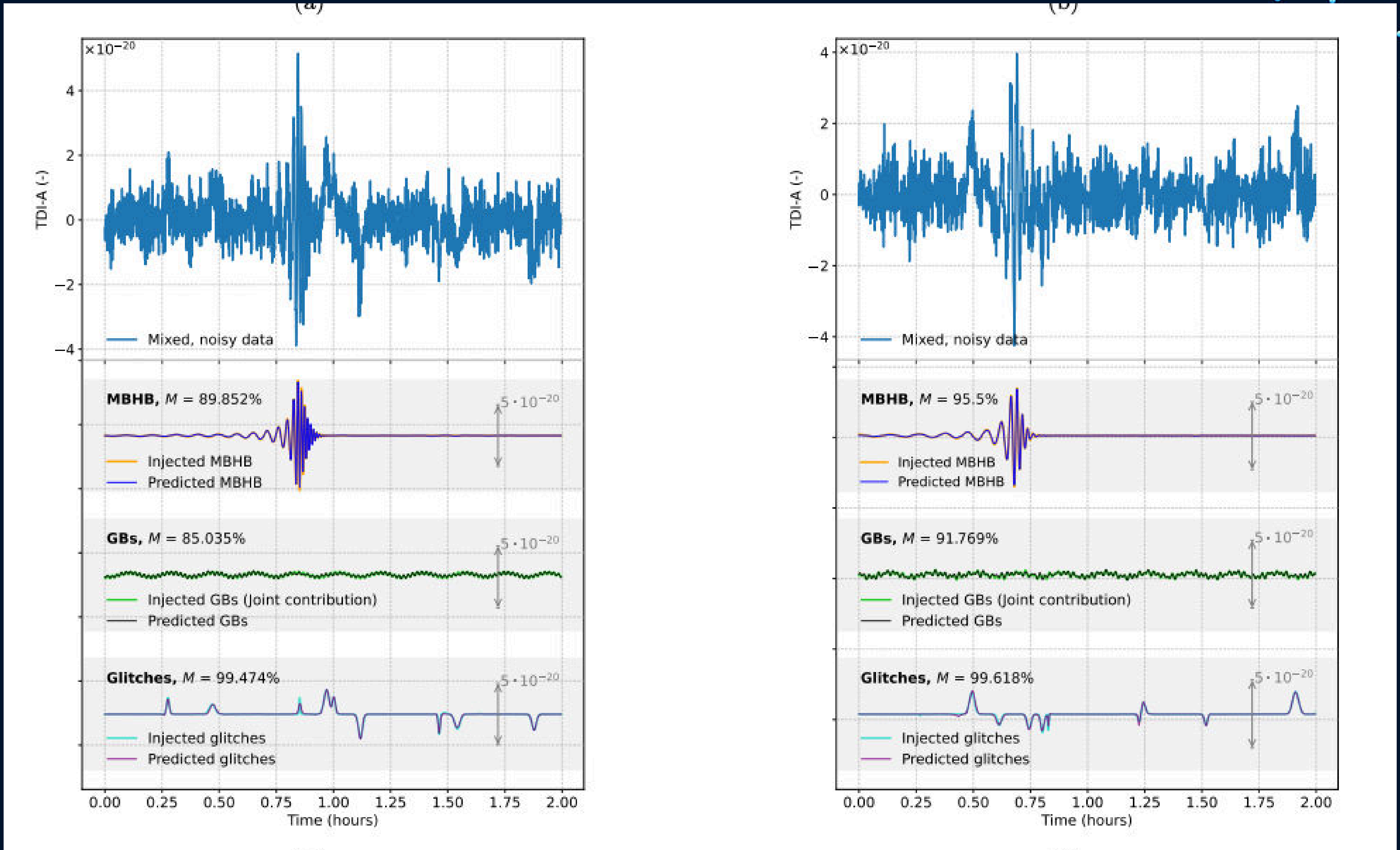

(c) (d)

when glitches occur during the MBHB ringdown

https://arxiv.org/pdf/2503.10398